Fractional Casson Blood Flow with Gold Nanoparticles (AuNPs) in a Slip Velocity Cylinder

Wan Faezah Wan Azmi, Ahmad Qushairi Mohamad*, Lim Yeou Jiann, Sharidan Shafie

Department of Mathematical Sciences, Faculty of Science, Universiti Teknologi Malaysia, 81310 Johor Bahru, Johor, Malaysia.

Abstract

The technology of nanofluid in the blood flow has attracted researchers to further study theoretically and experimentally due to its importance in treating the tumour and delivering the drugs effectively. Due to the lack of analytical study on nano-bloodfluid, this present paper aims to obtain an analytical solution of the Casson blood flow with gold nanoparticles in the cylinder with the free convection flow and slip velocity effect. The dimensionless governing equations are modelled with the Caputo-Fabrizio fractional derivative approach. Next, the joint methods of the Laplace transform and finite Hankel transform are used to obtain the analytical solution. The velocity profile increased as a fractional parameter, slip velocity parameter, nanoparticles volume fraction parameter and Grashof number are increased. Meanwhile, it decreased as the Casson parameter and Prandtl number increased. The temperature profile increased as the nanoparticle volume fraction parameter increased. However, it decreased as the Prandtl number increased. The obtained results are beneficial for the accuracy checking of the numerical methods. Besides, these results are significant to study the human blood flow behaviour with nanoparticles that help diagnose and treat the tumour cell.

Keywords   Casson blood flow, gold nanoparticles, Caputo-Fabrizio, slip velocity, finite Hankel transform

1.0 INTRODUCTION

Free convection flow is one of the heat transfer processes that occur naturally between surface and adjacent fluid. It happens due to the differences in temperature and density in the fluid. It attracts many researchers to study free convection flow in the cylinder due to its applications in engineering such as oil flow in the pipeline and biomedical fields such as human blood flow rates in the blood vessels. Additionally, the existence of the heat transfer process improves the homogeneity of the human blood concentration which controls the blood velocity in the drug delivery system [1]. Motivated by its wide applications, Khan *et al*., [2] analytically investigated the Newtonian fluid behaviour with the free convection flow in an oscillating cylinder. Similarly, Javaid *et al.,* [3] analytically studied the problem of free convection flow in an oscillating cylinder as Khan *et al*., [2] did, but with a different type of fluid, second-grade fluid. Moreover, fluid categories are also affecting fluid behaviour since the fluid is a heat carrier. In these studies, one of the famous non-Newtonian fluids, which is the Casson fluid model will be investigated. It behaves like an elastic solid if the condition of applied shear stress is greater than the yield stress, but it initiates the flow if the condition is inverse. Thus, based on its unique behaviour, it can imitate human blood flow in the small blood vessels [4]. Kumar and Rizvi [5] investigated Casson fluid flow in the moving cylinder with the effects of a free convective, chemical reaction and magnetic field. They numerically solved by using the Crank-Nicolson implicit finite difference method. They revealed that as the Casson parameter increased, the plasticity of the fluid decreased, hence, enhancing the fluid velocity.

Currently, many researchers gain interest in the Casson fluid model with the fractional derivative approach such as Caputo, Riemann-Liouville, Caputo-Fabrizio and Atangana-Baleanu. It is important for applications that are involved with

physical memory such as fluid mechanics applications. It discusses the *n*-notation of the derivative if it is a fractional or complex number [6]. Inspired by its importance, Ali *et al.*, [7] was among the earliest research group that analytically solved the Casson fluid flow in the fixed cylinder with Caputo fractional derivative approach. However, some fractional derivative models have limitations and are difficult to model complex physical problems due to the power law kernel. Hence, Caputo-Fabrizio fractional derivative model is one of the most suitable approaches to modeling the fluid flow problem since it has a non-singular kernel operator [8]. Then, Ali *et al.*, [9]–[11] encountered a similar problem as Ali *et al.*, [7] with the additional effect of the free convection flow in the cylinder. They solved the problem with the different boundary conditions such as fixed cylinder [9], moving cylinder [10] and oscillating cylinder [11]. They model the governing equations with the Caputo-Fabrizio fractional derivative approach. Later, Maiti *et al.*, [12]–[14] extended a similar problem with the additional effects of radiation and chemical reaction. All of them analytically solved the problems by using the joint methods Laplace transform and finite Hankel transform.

On the other hand, nanofluid is one of the innovative ideas to improve the heat transfer process of the fluid. Nanofluid is a fluid that consists of metallic nanometer-sized particles dispersed in the low thermal conductivity base fluid. It has been widely used in medical applications such as drug delivery and tumour treatment. Encouraged by its importance in improving fluid thermal conductivity [1], Ahmad *et al.*, [15] obtained an analytical solution for fractional Casson clay nanofluid with natural convection flow on the moving plate. They applied the Constant Caputo fractional derivative approach and solved the problem by using Laplace transform. Then, Sobamowo [16] extended a similar problem as Ahmad *et al.*, [15] numerically with additional effects of porosity, magnetic field, radiation and chemical reaction. Besides, Hamarsheh *et al.*, [17] investigated numerically free convection flow of carbon nanotubes dispersed in the Casson fluid past through a fixed circular cylinder. In this study, gold (Au) is considered a nanoparticle (NPs), which is dispersed uniformly in the human blood since it has good biocompatibility [18]. Imtiaz *et al.*,[19] explored the effect of the gold nanoparticles (Au NPs) dispersed in the human blood flow in the fixed cylinder with free convective heat transfer. They analytically solved by using Laplace and finite Hankel transform techniques together with the Caputo-Fabrizio fractional derivative approach. Nevertheless, none of them considered the slip velocity effect at the boundary.

By considering the slip velocity effect at the boundary, the problems can be modelled close to real-life applications such as blood flow in the arteries. It also plays a vital role in the variations of fluid velocity. It can be defined as a velocity gradient that occurs between two different mediums; a solid boundary and adjacent fluid flow on it [20]. Padma *et al.*, [21], [22] find out the fluid velocity with the presence of slip velocity is higher than the no-slip velocity at the boundary. They obtained an analytical solution for the Jeffrey fluid flow in the cylinder by using the combined methods of the Laplace transform and finite Hankel transform. Then, Afify [23] numerically discussed the effect of the slip boundary on the Casson nanofluid past through a sheet. Later, mathematical modelling has been numerically developed for the Casson nanofluid flow outside the stretching cylinder by Usman *et al.*, [24] and Tulu and Ibrahim[25]. Furthermore, Idowu *et al.*, [26] explored numerically the influence of slip velocity on the Casson nanofluid flow between two cylinders. However, their studies did not include the fractional derivative approach.

To the best of our knowledges, the impact of the slip velocity at the boundary together with the fractional derivative approach of Casson nanofluid in the cylindrical domain has not been investigated yet by the researchers. In this study, gold solid particles are considered nanoparticles and human blood is considered a base fluid with the Casson nanofluid model. It is a lack of clinical experiment research in the case of Au NPs since it consumes time and cost. Therefore, many researchers studied theoretically by using analytical and numerical methods. However, most of the researchers obtained results analytically by considering the no-slip velocity effect and fractional derivative approach. Thus, the present study aims to obtain and analyze the analytical solution of the unsteady free convection flow of Casson nanofluid with the Caputo-Fabrizio fractional derivative approach in the slip velocity cylinder. The momentum and energy governing equations are expressed in the Caputo-Fabrizio fractional derivative model. The analytical solutions for the velocity and temperature profiles are obtained by using the combined methods of the Laplace transform and finite Hankel transform. Then, the obtained analytical solution is plotted and analyzed graphically with the related parameters by using Maple software. The obtained results on the human blood behaviour either blood velocity or blood temperature with the various related parameters such as Au NPs concentration are beneficial for the study of a blood disease problem. For example, the obtained results of the human blood rates influence the speed of the Au NPs to be loaded to the desired tumour/cancerous tissues and maximize the damage of the cancerous cell.

2.0 MATHEMATICAL FORMULATION

Assume that an unsteady free convection flow of human blood dispersed with gold nanoparticles passed through an infinite vertical cylinder that reflects small blood vessels. Consider the radius of the cylinder as r_0, the axis along the horizontal direction is the *z*-axis and the *r*-axis which refers to the radial direction is taken normal to the *z*-axis. In this study, human blood will be modelled with the Casson fluid model. The nanofluid flow is driven by the buoyancy force and velocity gradient that occurred at the boundary of the cylinder. Initially at $t^*=0$, both nanofluid and cylinder are at rest condition with the ambient temperature T_∞. Then, nanofluid begins to flow due to the occurrence of slip velocity u_s at the boundary of the cylinder when $t^*>0$. Simultaneously, the cylinder temperature was raised to wall cylinder temperature, T_w and then it is maintained constant. The functions of fluid velocity and temperature are in terms of *r* and *t* only. **Figure 1** shows the diagram to describe and illustrate the physical problems.
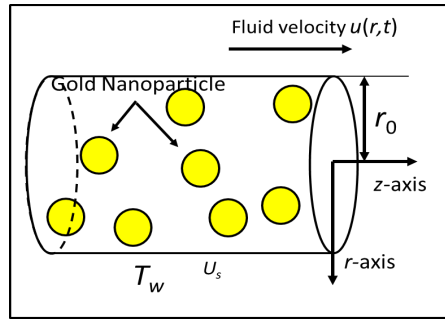
Figure 1 Physical problem illustration.

Based on Boussinesq's approximation and the Tiwari and Das nanofluid model, the governing equations of the momentum and energy for the present study are given as [19], [27]

$$\rho_{nf}\frac{\partial u^*(r,t)}{\partial t^*} = \mu_{nf}\left(1+\frac{1}{\beta}\right)\left(\frac{\partial^2 u^*(r,t)}{\partial r^{*2}}+\frac{1}{r^*}\frac{\partial u^*(r,t)}{\partial r^*}\right)+g\left(\rho\beta_T\right)_{nf}\left(T^*(r,t)-T_\infty\right) \tag{1}$$

$$\left(\rho C_p\right)_{nf}\frac{\partial T^*(r,t)}{\partial t^*} = k_{nf}\left(\frac{\partial^2 T^*(r,t)}{\partial r^{*2}}+\frac{1}{r^*}\frac{\partial T^*(r,t)}{\partial r^*}\right) \tag{2}$$

together with the related initial and boundary conditions

$$
\begin{aligned}
u^*(r^*,0)&=0 & T^*\left(r^*,0\right)&=T_\infty & &; \ r\in[0,r_0], \\
u^*(r_0^*,t^*)&=u_s^* & T^*\left(r_0^*,t^*\right)&=T_w & &; \ t^* > 0
\end{aligned}
\tag{3}
$$

where u^* is the velocity component along the *z*-axis, $\beta = \mu_B\sqrt{2\pi_c}/\tau_y$ is the Casson parameter, g is the gravitational acceleration and T^* is the temperature of the fluid. Moreover, the thermophysical properties in Casson nanofluids are involved with the effective density ρ_{nf}, effective dynamic viscosity μ_{nf}, thermal expansion coefficient $(\rho\beta_T)_{nf}$, effective heat capacity$(\rho c_p)_{nf}$, and effective thermal conductivity k_{nf} are defined as in equation (5). The effective thermal conductivity of the nanofluid is based on the Maxwell model which is only considered the spherical shape of nanoparticles according to Oztop *et al.* [28] and it is suitable for studying heat transfer enhancement by using nanofluids. Moreover, Brinkman highlighted that the viscosity of the nanofluid is approximated as the viscosity of a base fluid containing spherical particles [29]. Thus, the model is given as

$$
\begin{aligned}
\rho_{nf} &= \left(1-\phi\right)\rho_f + \phi\rho_s, \ \mu_{nf} = \frac{\mu_f}{\left(1-\phi\right)^{2.5}}, \ k_{nf} = k_f\left[\frac{k_s + 2k_f - 2\phi\left(k_f - k_s\right)}{k_s + 2k_f + \phi\left(k_f - k_s\right)}\right], \\
\left(\rho\beta_T\right)_{nf} &= \left(1-\phi\right)\left(\rho\beta_T\right)_f + \phi\left(\rho\beta_T\right)_s, \left(\rho C_p\right)_{nf} = \left(1-\phi\right)\left(\rho C_p\right)_f + \phi\left(\rho C_p\right)_s
\end{aligned}
\tag{5}
$$

where the subscript symbols *f* indicates fluid while *s* indicates solid and ϕ is the nanofluid solid volume fraction. The appropriate dimensionless variables are introduced as [11], [21]

$$t=\frac{t^*v}{r_0^2}, r=\frac{r^*}{r_0}, u=\frac{u^*}{u_0}, u_s=\frac{u_s^*}{u_0}, \theta=\frac{T-T_\infty}{T_w-T_\infty}. \tag{6}$$

The dimensionless variables substitute into Equations (1)-(3) to obtain governing equations and conditions in the dimensionless form. Besides, nanofluid model parameters are also substituted into the dimensionless governing equations and get

$$\frac{\partial u(r,t)}{\partial t} = M_3\beta_1\left(\frac{\partial^2 u(r,t)}{\partial r^2} + \frac{1}{r}\frac{\partial u(r,t)}{\partial r}\right) + M_4 Gr\theta(r,t), \tag{7}$$

$$\frac{\partial \theta(r,t)}{\partial t} = \frac{M_1}{M_2 \Pr}\left(\frac{\partial^2 \theta(r,t)}{\partial r^2} + \frac{1}{r}\frac{\partial \theta(r,t)}{\partial r}\right) \tag{8}$$

together with the related initial and boundary conditions

$$
\begin{aligned}
u(r,0)&=0, & \theta(r,0)&=0 & &; r \in [0,1], \\
u(1,t)&=u_s, & \theta(1,t)&=1 & &; t>0
\end{aligned}
\tag{9}
$$

where $M_3 = \dfrac{1}{(1-\phi)^{2.5}\left[(1-\phi)+\phi\rho_s/\rho_f\right]}$, $\beta_1 = \dfrac{1}{1+1/\beta}$, $M_4 = \dfrac{(1-\phi)\rho_f + \phi(\rho\beta_T)_s/(\beta_T)_f}{(1-\phi)\rho_f + \phi\rho_s}$, $M_2 = (1-\phi)+\dfrac{\phi(\rho c_p)_s}{(\rho c_p)_f}$,

$M_1 = \dfrac{k_s + 2k_f - 2\phi(k_f - k_s)}{k_s + 2k_f + \phi(k_f - k_s)}$,   are the constant parameters. Meanwhile, the obtained dimensionless parameters are

$Gr = \dfrac{g(\beta_T)_f(T_w - T_\infty)r_0^2}{v_f u_0}$ is the Thermal Grashof number and $\Pr = \dfrac{v_f(\rho c_p)}{k_f}$ is the Prandtl number. Later, Equations (7) and (8)

are applied Caputo-Fabrizio fractional derivative approach and obtained as

$$^{CF}D_t^\alpha u(r,t) = M_3\beta_1\left(\frac{\partial^2 u(r,t)}{\partial r^2} + \frac{1}{r}\frac{\partial u(r,t)}{\partial r}\right) + M_4 Gr\theta(r,t), \tag{10}$$

$$^{CF}D_t^\alpha \theta(r,t) = \frac{M_1}{M_2 \Pr}\left(\frac{\partial^2 \theta(r,t)}{\partial r^2} + \frac{1}{r}\frac{\partial \theta(r,t)}{\partial r}\right) \tag{11}$$

where $^{CF}D_t^\alpha f(r,t) = \dfrac{1}{1-\alpha}\displaystyle\int_0^\tau \exp\left(\frac{-\alpha(\tau-t)}{1-\alpha}\right)f'(\tau)dt$ for 0<α<1 is the definition of the Caputo-Fabrizio fractional derivative [12].

2.1 Problem Solution

The dimensionless forms of the governing equations solve by using the combined methods of the Laplace transform and finite Hankel transform. Both methods are very beneficial to obtain analytical solutions since the problems involve the cylindrical domain, transient and initial-boundary value problems.

2.2 Calculation of Temperature

Transformed equation (11) together with the associated initial and boundary conditions (9) by using Laplace transform technique, which yields

$$\frac{a_0 s\overline{\theta}(r,s)}{s+a_1} = \frac{M_1}{M_2 \Pr}\left[\frac{\partial^2 \overline{\theta}(r,s)}{\partial r^2} + \frac{1}{r}\frac{\partial \overline{\theta}(r,s)}{\partial r}\right], \tag{12}$$

$$\overline{\theta}(1,s) = \frac{1}{s},$$
(13)

where $a_0 = 1/1-\alpha$, and $a_1 = a_0\alpha$, are the fractional constant parameters, $\overline{\theta}(r,s)$ is the Laplace transform of the function $\theta(r,t)$ and s is the transformation variable. Later, Laplace's partial differential equation (12) transforms into the ordinary differential equation with respect to the radial coordinate by using finite Hankel transform of zero-order together with the related condition (13), giving

$$\overline{\theta}_H(r_n,s) = \frac{M_5 r_n J_1(r_n)}{s}\left[\frac{s+a_1}{a_4[n]s+a_3[n]}\right],$$
(14)

where $\overline{\theta}_H(r_n,s) = \int_0^1 r\overline{\theta}(r,s)J_0(rr_n)\,dr$ is the finite Hankel transform of the function $\overline{\theta}(r,s)$ and r_n with $n=0,1,...$ are the positive roots of the equation $J_0(x) = 0$, where J_0 is being the Bessel function of the first kind and zero-order, J_1 is the Bessel function of the first kind and first order. Besides, $M_5 = M_1/M_2$, $a_4[n] = a_0\Pr + M_5 r_n^2$, and $a_3[n] = a_1 M_5 r_n^2$ are the constant parameters. Then, equation (14) is simplified and obtained as

$$\overline{\theta}_H(r_n,s) = \frac{J_1(r_n)}{r_n}\left[\frac{1}{s} - \frac{a_0\Pr}{(s+a_5[n])(a_4[n])}\right],$$
(15)

where $a_5[n] = a_3[n]/a_4[n]$ is the constant parameter. After that, the inverse Laplace transform is applied to the equation (15), attaining as

$$\theta_H(r_n,t) = \frac{J_1(r_n)}{r_n}\left[1 - \frac{a_0\Pr\exp(-a_5[n]t)}{a_4[n]}\right].$$
(16)

Finally, the analytical solution of temperature profiles is obtained by applying the inverse finite Hankel transform to the equation (16) and gaining as

$$\theta(r,t) = 1 - 2a_0\Pr\sum_{n=1}^{\infty}\frac{J_0(rr_n)\exp(-a_5[n]t)}{r_n J_1(r_n)a_4[n]}.$$
(17)

2.3 Calculation of Velocity

By applying Laplace transform technique to equation (10) together with the related initial and boundary conditions (7), get

$$\frac{a_0 s\overline{u}(r,s)}{s+a_1} = M_3\beta_1\left[\frac{\partial^2\overline{u}(r,s)}{\partial r^2} + \frac{1}{r}\frac{\partial\overline{u}(r,s)}{\partial r}\right] + M_4 Gr\overline{\theta}(r,s),$$
(18)

$$\overline{u}(1,s) = \frac{u_s}{s},$$
(19)

where $\overline{u}(r,s)$ is the Laplace transform of the function $u(r,t)$. Then, apply finite Hankel transform into equation (18) together with the boundary condition (19) to obtain an ordinary differential equation (ODE) as

$$\overline{u}_H(r_n,s) = \left(M_3\beta_1 r_n J_1(r_n)\frac{u_s}{s} + M_4 Gr\overline{\theta}_H(r_n,s)\right)\left(\frac{s+a_1}{(a_0+M_3\beta_1 r_n^2)s+a_1 M_3\beta_1 r_n^2}\right),$$
(20)

where $\overline{u}_H(r_n,s) = \int_0^1 r\overline{u}(r,s)J_0(rr_n)\,dr$ is the finite Hankel transform of the function $\overline{u}(r,s)$. Equation (20) can be written

in the simplification form as

$$\overline{u}_H(r_n,s) = F_1(s) + F_2(s) - F_3(s),$$

(21)

With

$$F_1(s) = \frac{J_1(r_n)}{r_n}\left[\frac{u_s}{s} - \frac{a_0 u_s}{(s+a_8[n])a_6[n]}\right], \quad F_2(s) = \frac{J_1(r_n)}{r_n^3}\frac{M_4 Gr}{M_3\beta_1}\left[\frac{1}{s} - \frac{a_0}{a_6[n](s+a_8[n])}\right],$$

$$F_3(s) = \frac{J_1(r_n)}{r_n^3}\frac{M_4 Gr a_0 \Pr}{(M_3\beta_1 \Pr - M_5)}\left[\frac{\Pr}{a_4[n](s+a_5[n])} - \frac{1}{a_7[n](s+a_8[n])}\right].$$

Where $a_6[n] = a_1 M_3\beta_1 r_n^2$, $a_7[n] = a_0 + M_3\beta_1 r_n^2$ and $a_8[n] = a_6[n]/a_7[n]$ are the constant parameters. Next, equation (21) transforms from the *s*-domain into the *t*-domain by using the inverse Laplace transform, getting as

$$u_H(r_n,t) = f_1(t) + f_2(t) - f_3(t),$$

(22)

with

$$f_1(t) = \frac{J_1(r_n)}{r_n}\left(u_s - \frac{a_0 u_s}{a_7[n]}\exp(-a_8[n]t)\right), \quad f_2(t) = \frac{J_1(r_n)}{r_n^3}\frac{M_4 Gr}{M_3\beta_1}\left[1 - \frac{a_0\exp(-a_8[n]t)}{a_7[n]}\right],$$

$$f_3(t) = \frac{J_1(r_n)}{r_n^3}\frac{M_4 Gr a_0 \Pr}{(M_3\beta_1 \Pr - M_5)}\left[\frac{\Pr\exp(-a_5[n]t)}{a_4[n]} - \frac{\exp(-a_8[n]t)}{a_7[n]}\right].$$

Lastly, use inverse finite Hankel transform to obtain the analytical solution of the nanofluid velocity, given as

$$u(r,t) = u_s - 2a_0 u_s \sum_{n=1}^{\infty}\frac{J_0(rr_n)}{r_n J_1(r_n)}\frac{\exp(-a_8[n]t)}{a_7[n]}$$

$$+ \frac{2M_4 Gr}{M_3\beta_1 \Pr - M_5}\sum_{n=1}^{\infty}\frac{J_0(rr_n)}{r_n^3 J_1(r_n)}\left[\begin{array}{c}\dfrac{M_3\beta_1 \Pr - M_5}{M_3\beta_1} + \dfrac{a_0 M_5\exp(-a_8[n]t)}{a_7[n]M_3\beta_1} \\ - \dfrac{a_0 \Pr^2\exp(-a_5[n]t)}{a_4[n]}\end{array}\right].$$

(23)

3.0 RESULTS AND DISCUSSIONS

In order to validate the obtained present result, the limiting case of the obtained present result as in equation (23) is compared with the previously published result by Khan *et al.*, [2]. Based on the graph observation in **Figure 2**, both graphs are identical which shows they are in mutual agreement. Thus, the obtained analytical solution is accurate.
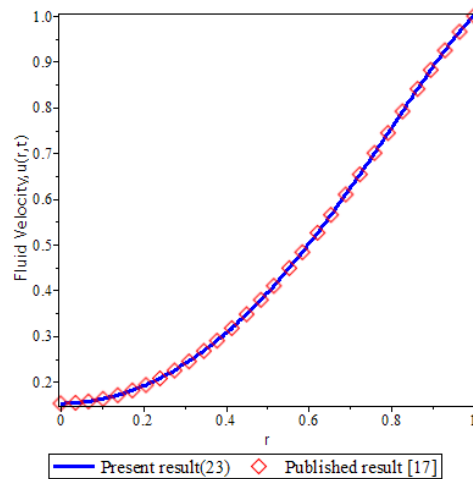
Figure 2 Comparison of velocity profile $u(r,t)$ from equation (23) when $\beta \to \infty$, u_s=1.0, α=0.999, ϕ =0 with equation (29) when ω= 0 by Khan et al. [1].

In this study, the analytical solutions of nanofluid velocity and temperature in equations (17) and (23) are graphically plotted to analyse and understand the nanofluid flow behaviour. It involves important parameters such as Casson parameter β, Grashof number Gr, Prandtl number Pr, slip velocity parameter u_s, fractional parameter α, nanoparticles volume fraction ϕ and time parameter t. The influences of the parameters on the nanofluid flow behaviour are displayed in **Figures 3-10**.

The effects of the Casson parameter on the fluid velocity are displayed in **Figure 3**. As we can see, fluid velocity decreases as the Casson parameter increases with the presence of slip velocity and no-slip velocity at the wall of the cylinder. When the Casson parameter increases, it leads to an increase in fluid viscosity and internal friction. As result, the fluid becomes thicker and decrement in fluid velocity.

Figure 4 presents the influence of the Grashof number on the fluid velocity with the existence of the slip and no-slip velocity effect at the boundary. It is found that an increment of the Grashof number leads to an increment in the fluid velocity. During free convection flow, the buoyancy force is dominant. Fluid particles near the boundary will circulate due to the density difference which results from the temperature gradient. Thus, as the Grashof number increase, buoyancy force will increase and enhance the fluid flow movement.

Meanwhile, fluid velocity and temperature decrease with the increases of the Prandtl number as shown in **Figures 5-6**. As the Prandtl number increases, momentum diffusivity increases. It causes momentum to spread between the particles to increase and resist the motion between the fluid particles. Thus, the fluid velocity decrease. Meanwhile, thermal diffusivity is inversely related to the Prandtl number. A larger Prandtl number causes fluid to cool down faster. Hence, fluid temperature decreases as the Prandtl number increases.

The impacts of nanoparticle volume fraction on the fluid velocity and temperature are illustrated in **Figures 7-8**. The velocity and temperature of the pure blood without nanoparticles (ϕ=0) are lower than the blood with gold nanoparticles. It shows that adding the nanoparticles can enhance the thermal conductivity of the nanofluid. Based on the graph observation also shows that increasing the nanoparticles volume fraction, will enhance the blood velocity and temperature. It is due to the natural convective heat transfer among the nanoparticles in blood flow increases as the nanoparticle volume fraction increases. Thus, it increases the motion of the nanoparticles in the blood flow. Consequently, the velocity and temperature of the nanofluid increase.

Besides, the fractional parameter also affects fluid velocity and temperature as depicted in **Figures 9-10**. By increasing the fractional parameter (0 <α<1), fluid velocity and temperature increase with the presence of slip and no-slip velocity in a large time interval (t>2). Conversely, fluid temperature decreases as the fractional parameter increases for a small-time interval (t=0.5). The differences occur between small-time and large-time intervals due to the memory effect of the fractional derivative. In addition, it is shown that the increment of the fluid with the fractional model is more realistic compared with the classical model (α=1).

Moreover, the slip velocity effect at the boundary also contributes to the increment of the fluid velocity at the wall of the cylinder (r=1) as revealed in **Figures 3-5,7,9**. It is due to the occurrence of velocity gradient between two different mediums, for this study involves the fluid flow and wall of the cylinder(solid). Thus, fluid velocity flow near r=1 will be the same as the slip velocity occurring at r=1. Besides, fluid velocity increases when approaching the center of the cylinder (r=0) as time increases. Furthermore, the slip velocity effect will be considered in this study since it exists in real-life applications such as blood flow in the arteries.
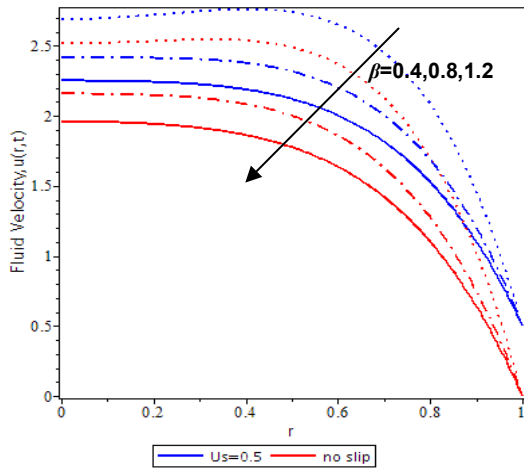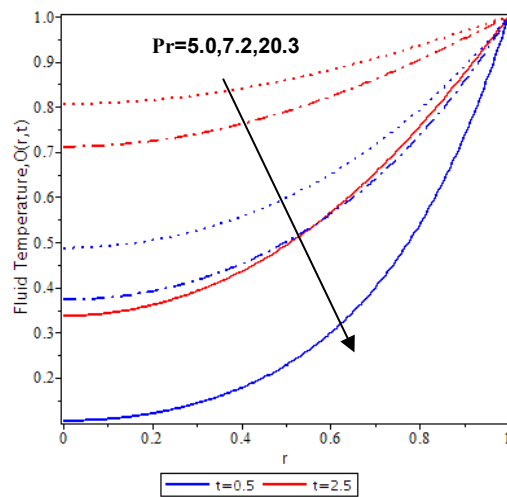
Figure 3. Fluid velocity $u(r,t)$ with various of Casson parameter when α=0.5, Gr=1, Pr=20.3, ϕ=0.2 and t=2.
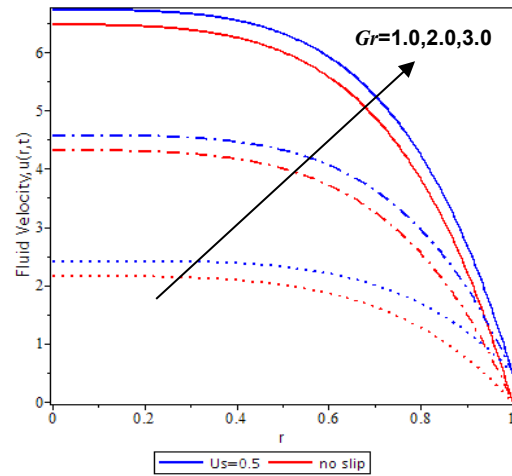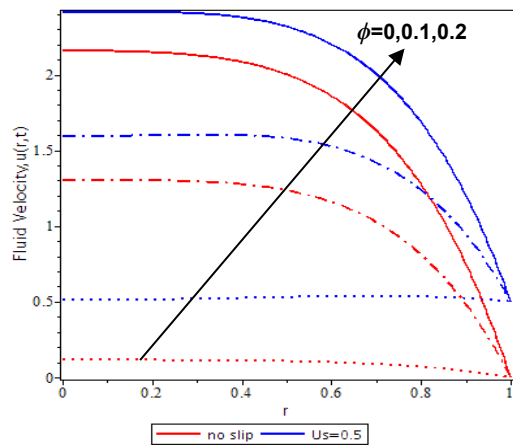

Figure 4. Fluid velocity $u(r,t)$ with various of Grashof number when α=0.5, β=0.8, Pr=20.3, ϕ=0.2 and t=2.
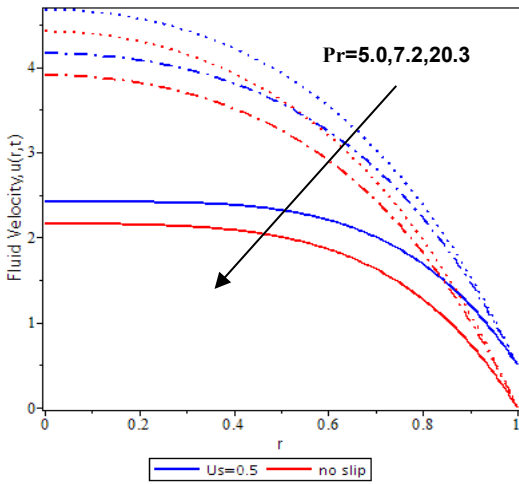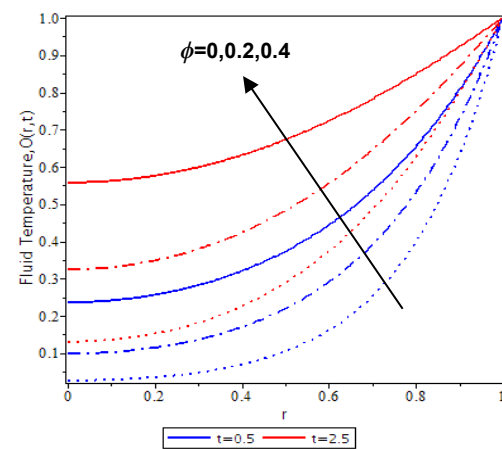

Figure 5. Fluid velocity $u(r,t)$ with various of Prandtl number when α=0.5, Gr=1, β=0.8, ϕ=0.2 and t=2.

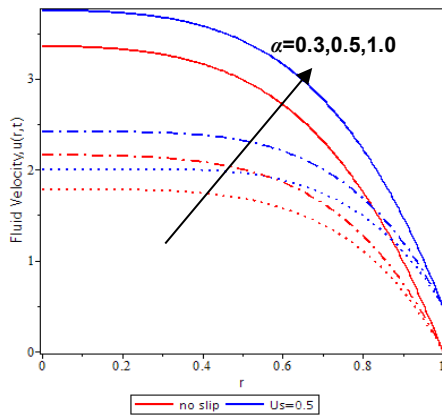**Figure 6.** Fluid temperature $\theta(r,t)$ with various Prandtl number when α=0.5, Gr=1 and ϕ=0.2.

Figure 7. Fluid velocity $u(r,t)$ with various of nanoparticles volume fraction when α=0.5, Gr=1, β=0.8, Pr=20.3 and t=2.

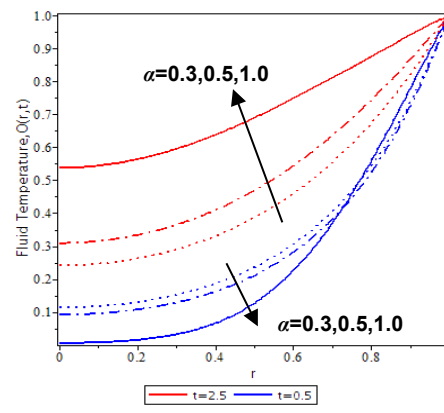**Figure 8.** Fluid temperature $\theta(r,t)$ with various nanoparticles volume fractions when α=0.5, Gr=1 and Pr=20.3.

Figure 9. Fluid velocity $u(r,t)$ with various of fractional parameter when Gr=1, β=0.8, Pr=20.3, ϕ=0.2 and t=2.

Figure 10. Fluid temperature $\theta(r,t)$ with various of fractional parameter when ϕ=0.2, Gr=1, Pr=20.3

4.0 CONCLUSION

In conclusion, the unsteady free convection flow of blood with Au NPs past through a cylinder together with the slip velocity effect has been investigated. The governing equations are modelled with the Caputo-Fabrizio fractional derivatives approach. Then, the analytical solutions of the velocity and temperature profiles are obtained by using the joint methods of the Laplace transform and finite Hankel transform. The findings obtained are as below;

  i.   The limiting case of the obtained analytical solution is matching the previously published result. Thus, the obtained solution is accepted.
  ii.   Fluid velocity increases with the presence of u_s, Gr, ϕ, α and t.
  iii.   Decrement of fluid velocity as increases values of β, and Pr.
  iv.   Fluid temperature decreases as Pr increases while fluid temperature increases as ϕ and t increase.
  v.   The fractional parameter increases lead to an increase in fluid temperature for a larger time interval and vice versa.
  vi.   The fractional fluid model is more realistic than the classical fluid model.
  vii.   Slip velocity enhances the fluid flow, especially at r=1.
  viii.   Au NPs increase human blood flow and thermal conductivity.

The findings are very useful to study the human blood behavior in the small arteries to diagnose and treat any related blood diseases and tumors. For example, in a drug delivery system, as fluid temperature increased, the concentration of the human blood flow with Au NPs reduced which caused an increment of the human blood flow. Hence, the anticancer drug is released faster at the desired cancerous cell.

Acknowledgment

References

[1]   M. Sheikhpour, M. Arabi, A. Kasaeian, A. R. Rabei, and Z. Taherian, "Role of nanofluids in drug delivery and biomedical technology: Methods and applications," *Nanotechnol. Sci. Appl.*, vol. 13, pp. 47–59, 2020.

[2]   I. Khan, N. A. Shah, A. Tassaddiq, N. Mustapha, and S. A. Kechil, "Natural convection heat transfer in an oscillating vertical cylinder," *PLoS One*, vol. 13, no. 1, p. e0188656, Jan. 2018.

[3]   M. Javaid, M. Imran, M. A. Imran, I. Khan, and K. S. Nisar, "Natural convection flow of a second grade fluid in an infinite vertical cylinder," *Sci. Rep.*, pp. 1–11, 2020.

[4]   R. P. Chhabra, "Non-Newtonian Fluids : An Introduction," in *SERC School-cum-Symposium on Rheology of complex fluids*, 2010, pp. 1–33.

[5]   G. Kumar and S. M. . Rizvi, "Casson fluid flow past on vertical cylinder in the presence of chemical reaction and magnetic field," *Appl. Appl. Math. An Int. J.*, vol. 16, no. 1, pp. 524–537, 2021.

[6]   S. S. Ray, A. Atangana, S. C. O. Noutchie, M. Kurulay, N. Bildik, and A. Kilicman, "Fractional calculus and its applications

in applied mathematics and other sciences," *Math. Probl. Eng.*, vol. 2014, pp. 2–4, 2014.

[7]   F. Ali, N. A. Sheikh, I. Khan, and M. Saqib, "Magnetic field effect on blood flow of Casson fluid in axisymmetric cylindrical tube: A fractional model," *J. Magn. Magn. Mater.*, vol. 423, no. May 2016, pp. 327–336, 2017.

[8]   A. Shaikh, A. Tassaddiq, K. S. Nisar, and D. Baleanu, "Analysis of differential equations involving Caputo–Fabrizio fractional operator and its applications to reaction–diffusion equations," *Adv. Differ. Equations*, vol. 2019, no. 1, 2019.

[9]   F. Ali, A. Imtiaz, I. Khan, and N. A. Sheikh, "Flow of magnetic particles in blood with isothermal heating: A fractional model for two-phase flow," *J. Magn. Magn. Mater.*, vol. 456, pp. 413–422, 2018.

[10]   F. Ali, A. Imtiaz, I. Khan, and N. A. Sheikh, "Hemodynamic flow in a vertical cylinder with heat transfer: Two-phase caputo fabrizio fractional model," *J. Magn.*, vol. 23, no. 2, pp. 179–191, 2018.

[11]   F. Ali, N. Khan, A. Imtiaz, I. Khan, and N. A. Sheikh, "The impact of magnetohydrodynamics and heat transfer on the unsteady flow of Casson fluid in an oscillating cylinder via integral transform: A Caputo–Fabrizio fractional model," *Pramana - J. Phys.*, vol. 93, no. 3, pp. 1–12, 2019.

[12]   S. Maiti, S. Shaw, and G. C. Shit, "Caputo–Fabrizio fractional order model on MHD blood flow with heat and mass transfer through a porous vessel in the presence of thermal radiation," *Phys. A Stat. Mech. its Appl.*, vol. 540, p. 123149, 2020.

[13]   S. Maiti, S. Shaw, and G. C. Shit, "Fractional order model of thermo-solutal and magnetic nanoparticles transport for drug delivery applications," *Colloids Surfaces B Biointerfaces*, vol. 203, no. March, p. 111754, 2021.

[14]   S. Maiti, S. Shaw, and G. C. Shit, "Fractional order model for thermochemical flow of blood with Dufour and Soret effects under magnetic and vibration environment," *Colloids Surfaces B Biointerfaces*, vol. 197, no. October 2020, p. 111395, 2021.

[15]   M. Ahmad, I. Asjad, A. Akg, and D. Baleanu, "Analytical solutions for free convection flow of Casson nanofluid over an infinite vertical plate," *AIMS Math.*, vol. 6, no. 3, pp. 2344–2358, 2020.

[16]   M. G. Sobamowo, "Transient free convection heat and mass transfer of Casson nanofluid over a vertical porous plate subjected to magnetic field and thermal radiation," *Eng. Appl. Sci. Lett.*, vol. 3, no. 2, pp. 9–18, 2020.

[17]   A. S. Hamarsheh, F. A. Alwawi, H. T. Alkasasbeh, A. M. Rashad, and R. Idris, "Heat Transfer Improvement in MHD Natural Convection Flow of Graphite Oxide / Carbon Nanotubes-Methanol Based Casson Nanofluids past a Horizontal Circular Cylinder," *Processes*, vol. 8, no. 11, p. 1444, 2020.

[18]   A. Ghadimi, R. Saidur, and H. S. C. Metselaar, "A review of nanofluid stability properties and characterization in stationary conditions," *Int. J. Heat Mass Transf.*, vol. 54, no. 17–18, pp. 4051–4068, 2011.

[19]   A. Imtiaz, O. M. Foong, A. Aamina, N. Khan, F. Ali, and I. Khan, "Generalized model of blood flow in a vertical tube with suspension of gold nanomaterials: Applications in the cancer therapy," *Comput. Mater. Contin.*, vol. 65, no. 1, pp. 171–192, 2020.

[20]   Y. Nubar, "Blood Flow, Slip, and Viscometry," *Biophys. J.*, 1971.

[21]   R. Padma, R. T. Selvi, and R. Ponalagusamy, "Effects of slip and magnetic field on the pulsatile flow of a Jeffrey fluid with magnetic nanoparticles in a stenosed artery," *Eur. Phys. J. Plus*, vol. 134, pp. 1–15, 2019.

[22]   R. Padma, R. Ponalagusamy, and R. Tamil Selvi, "Mathematical modeling of electro hydrodynamic non-Newtonian fluid flow through tapered arterial stenosis with periodic body acceleration and applied magnetic field," *Appl. Math. Comput.*, vol. 362, p. 124453, 2019.

[23]   A. A. Afify, "The Influence of Slip Boundary Condition on Casson Nanofluid Flow over a Stretching Sheet in the Presence of Viscous Dissipation and Chemical Reaction," *Math. Probl. Eng.*, vol. 2017, 2017.

[24]   M. Usman, F. Ahmed, R. UI, W. Wang, and O. Defterli, "Thermal and velocity slip effects on Casson nanofluid flow over an inclined permeable stretching cylinder via collocation method," *Int. J. Heat Mass Transf.*, vol. 122, pp. 1255–1263, 2018.

[25]   A. Tulu and W. Ibrahim, "Spectral relaxation method analysis of Casson nanofluid flow over stretching cylinder with variable thermal conductivity and Cattaneo – Christov heat flux model," *Heat Transf.*, no. December 2019, pp. 1–23, 2020.

[26]   A. S. Idowu, M. T. Akolade, J. U. Abubakar, and T. L. Oyekunle, "Nonlinear convection flow of dissipative Casson nanofluid through an inclined annular microchannel with a porous medium," *Heat Transf.*, no. September, pp. 1–19, 2020.

[27]   W. N. in N. Noranuar, A. Q. Mohamad, S. Shafie, I. Khan, L. Y. Jiann, and M. R. Ilias, "Non-coaxial rotation flow of MHD Casson nanofluid carbon nanotubes past a moving disk with porosity effect," *Ain Shams Eng. J.*, vol. 12, no. 4, pp. 4099-4110, 2021.

[28]   H. F. Oztop and E. Abu-Nada, "Numerical study of natural convection in partially heated rectangular enclosures filled with nanofluids," *Int. J. Heat Fluid Flow*, vol. 29, no. 5, pp. 1326–1336, 2008.

[29]   J. Tripathi, B. Vasu, R. S. R. Gorla, A. J. Chamkha, P. V. S. N. Murthy, and O. A. Bég, "Blood flow mediated hybrid nanoparticles in human arterial system: Recent research, development and applications," *J. Nanofluids*, vol. 10, no. 1, pp. 1–30, 2021.